

# Numerical Simulations of n-Type Optoelectronic Devices with Single-Band Effective Mass Hamiltonian

Nonequilibrium Green's function approach

Andrzej Kolek

Department of Electronics Fundamentals  
Rzeszów University of Technology  
Rzeszów, Poland  
akoleknd@prz.edu.pl

**Abstract**—One-band 1D effective mass model useful in the simulations of layered n-type devices is proposed. The model preserves nonparabolicity both in transport and in-plane directions and enables calculations of intersubband absorption. Simulations of quantum cascade laser are presented which use the model within nonequilibrium Green's function method.

**Keywords**—one-band effective mass approximation, in-plane dispersion, nonequilibrium Green's function, quantum cascade laser, intersubband absorption.

## I. INTRODUCTION

Single-band effective mass equation (EME) is a simple and useful description of electronic properties of unipolar devices. For optoelectronic devices utilizing optical transition between energy levels far from the band edge, this treatment occurs insufficient due to the influence of remote bands. Multiband  $\mathbf{k}\cdot\mathbf{p}$  Hamiltonians are then necessary, which are more complex and hardly useable when self-consistent solutions taking into account multiple scattering mechanisms are required. For this reasons, various modifications of EME are proposed in order to enhance device's physics description maintaining the benefit relating on one-band treatment. One of them is 1D equation

$$\frac{-\hbar^2}{2} \frac{d}{dz} \frac{1}{m(E,z)} \frac{df}{dz} + \left( E_c(z) + \frac{\hbar^2 k^2}{m(E,z)} \right) f = E f, \quad (1)$$

which can be used to model n-type layered devices. It uses isotropic (bulk) energy dependent effective mass (EDEM) both in longitudinal ( $z$ ) and in-plane kinetic energy terms. Equation (1) was shown to reproduce well the in-plane nonparabolicity predicted by  $8 \times 8 \mathbf{k}\cdot\mathbf{p}$  description [1] and was successfully applied to model quantum cascade lasers (QCLs) utilizing intersubband transitions in the conduction band [1],[2]. The solutions of (1) are, however, not orthonormal what rises the problems connected with correct evaluation of the momentum matrix elements. They cannot be overcome by completing the functions  $f(z)$  with fictitious valence band components  $g(z)$ , as proposed in [3],[4] because the two-band counterpart of (1) is still energy dependent and do not provide orthogonal states. In

the paper another effective mass approximation is proposed which also reproduces  $8 \times 8 \mathbf{k}\cdot\mathbf{p}$  in-plane dispersion well and simultaneously reduces to longitudinal Hamiltonian which has energy independent two-band counterpart. Then, intersubband absorption can be rigorously treated as described in [3],[4]. This model is used with nonequilibrium Green's function (NEGF) method to simulate QCL emitting at  $\sim 5 \mu\text{m}$ . In this device the transitions occur between the states which are more than 0.25 eV above conduction band edge so that accounting somehow for nonparabolicity is mandatory for quantity-aimed analyses.

## II. ANISOTROPIC NONPARABOLICITY

Instead of (1), one may consider

$$\frac{-\hbar^2}{2} \frac{d}{dz} \frac{1}{m(E_z, z)} \frac{df}{dz} + E_c(z) f = E_z f \quad (2a)$$

$$E_z = E - \frac{\hbar^2 k^2}{m(E, z_{aw})}, \quad (2b)$$

where different effective masses are used in transport and in-plane directions. The dispersion relation for the in-plane vector  $k$ , obtained for an exemplary quantum well by inserting  $m(E, z) = m^*(z) \{1 + [E - E_c(z)]/E_g(z)\}$  into (2b), is shown in Fig. 1. As can be seen, the deviation from  $8 \times 8 \mathbf{k}\cdot\mathbf{p}$  prediction for lower state is even smaller than that for (1). However, there is no evidence which approximation is better because  $8 \times 8 \mathbf{k}\cdot\mathbf{p}$  is also an approximation which introduces errors at high- $k$  values.

The subscript 'aw' in (2b) abbreviates 'active wells' so,  $z_{aw}$  points at the wells where major optical transition takes place. Fixing  $z$  at  $z_{aw}$  in (2b) makes  $E_z$  loose its spatial dependence and then (2a) takes the usual form of energy-dependent EME [3],[4]. Equation (2a) provides longitudinal solutions  $f(z)$  which are still non-orthogonal, however, unlike in (1), orthonormality can be easily recovered evaluating fictitious valence terms [3]

$$g(z) = -\frac{m^* \sqrt{\gamma}}{m(E_z, z)} \frac{df(z)}{dz}.$$

The work was supported by Polish National Center for Research and Development (NCBR) under grant PBS 1/B3/2/2012 (EDEN).

Two-component wave functions ( $f$ ,  $g$ ) form orthonormal set which can be used in the calculations of momentum matrix elements [3],[4].

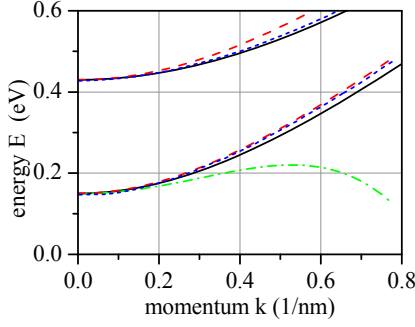


Fig. 1. In-plane dispersion calculated for (1) - solid, or (2) - dashed, for 4.8 nm wide InGaAs/AlInAs quantum well (lattice matched to InP) compared to  $8 \times 8$   $kp$  calculations in [1] (dotted) and  $14 \times 14$   $kp$  model (dash-dotted) of [5].

### III. NEGF IMPLEMENTATION

Equation (2) defines the  $k$ -dependent Hamiltonian which can be used in NEGF method. In the real space implementation of [2], the conduction band Green's functions (GFs)  $G^R$ ,  $G^<$ , are the four-parameter functions of positions  $z$ ,  $z'$ , energy  $E$ , and momentum modulus  $k$ . They can be found in self-consistent solution of Dyson, Keldysh and Poisson equations that involve scatterings and coupling to the leads through appropriate self-energies. In the iteration procedure virtual valence components (index  $v$ ) of GFs (equivalent to eigenfunctions components  $g$ ) should be evaluated as they contribute to densities of states (DOS) and electrons (DOE)

$$N(E, k, z) = -\frac{1}{\pi a} \text{Im}(G^R(E, k, z, z) + G_v^R(E, k, z, z)),$$

$$n(E, k, z) = -\frac{i}{2\pi a} (G^<(E, k, z, z) + G_v^<(E, k, z, z)),$$

and so influence the self-consistent solution through Poisson equation. For discretized Hamiltonians, useful in numerical simulations and offering compact form of integral equations, the retarded GF valence component is given by [6]

$$\mathbf{G}_{vc}^R(E, k) = (E_z - \mathbf{E}_v)^{-1} \mathbf{H}_{cv}^t \mathbf{G}^R(E, k),$$

$$\mathbf{G}_v^R(E, k) = (E_z - \mathbf{E}_v)^{-1} [\mathbf{I} + \mathbf{H}_{cv}^t \mathbf{G}_{vc}^R(E, k)].$$

where  $\mathbf{H}_{cv}$  is the discretized differential operator

$$\frac{\hbar^2}{2m^* \sqrt{\gamma}} \frac{d}{dz} \rightarrow \mathbf{H}_{cv}, \text{ and } E_g(z) - E_g(z) = E_v(z) \rightarrow \mathbf{E}_v.$$

Valence components of lesser Green's function can be obtained from the matrix equation

$$\begin{bmatrix} \mathbf{G}^< & \mathbf{G}_{cv}^< \\ \mathbf{G}_{vc}^< & \mathbf{G}_v^< \end{bmatrix} = \begin{bmatrix} \mathbf{G}^R \mathbf{\Sigma}^< \mathbf{G}^{R*} & \mathbf{G}^R \mathbf{\Sigma}^< \mathbf{G}_{vc}^{R*} \\ \mathbf{G}_{vc}^R \mathbf{\Sigma}^< \mathbf{G}^{R*} & \mathbf{G}_{vc}^R \mathbf{\Sigma}^< \mathbf{G}_{vc}^{R*} \end{bmatrix},$$

where  $\mathbf{\Sigma}^<$  is the lesser self-energy. Eventually, the optical gain can be evaluated making use of the formulation in [7] applied to two-band Hamiltonian, as in [6].

### IV. QCL SIMULATIONS

Equation (2) was used with the NEGF implementation of Sec. III to calculate electronic transport and optical gain in QCL design of [8]. In Fig. 2, which shows sample results, focus is paid on  $k$ -resolved quantities which demonstrate in-plane nonparabolicity contained in the model. Preserving this feature is crucial for realistic modeling of intersubband gain. As discussed in [9], in these devices gain can emerge due to local (in  $k$ -space) population inversion, which is not destroyed by high- $k$  absorption due to inherent in-plane nonparabolicity.

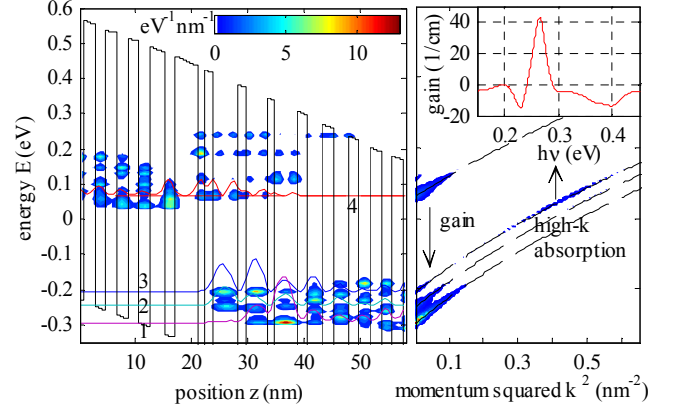


Fig. 2. (a) Spectral function at  $k = 0$ , and (b) subband occupation in active wells of  $5 \mu\text{m}$  2-phonon resonance QCL design of [8]. Population inversion is observed only at low- $k$  momenta where the occupation of upper laser subband 4 exceeds the occupation of lower laser subband 3.  $4 \rightarrow 3$  transitions at high- $k$  values, where the occupation is normal, do not destroy gain because they absorb photons with lower energy:  $\hbar v_{\text{high-}k} < \hbar v_{\text{low-}k}$ . These transitions burn a hole in front of the gain peak in the gain spectrum as shown in the inset.

### REFERENCES

- [1] J. Faist, *Quantum Cascade Lasers*, Oxford University Press, Oxford, 2013.
- [2] T. Kubis, C. Yeh, and P. Vogl, "Theory of nonequilibrium quantum transport and energy dissipation in terahertz quantum cascade lasers," *Phys. Rev. B*, vol. 79, no. 19, art. no. 195323, May 2009.
- [3] R. P. Leavitt, "Empirical two-band model for quantum wells and superlattices in an electric field," *Phys. Rev. B* vol. 44, pp.11270-11280, Nov. 1991.
- [4] C. Sirtori, F. Capasso, J. Faist, and S. Scandolo, "Nonparabolicity and a sum rule associated with bound-to-bound and bound-to-continuum intersubband transitions in quantum wells," *Phys. Rev. B*, vol. 50, no. 12, pp. 8663-8674, Sept. 1994.
- [5] U. Ekenberg, "Nonparabolicity effects in quantum well: Sublevel shift, parallel mass, and Landau levels," *Phys. Rev. B*, vol. 40, pp. 7714-7726, Oct. 1989.
- [6] A. Kolek, "Nonequilibrium Green's function formulation of intersubband absorption for nonparabolic single-band effective mass Hamiltonian," *Appl. Phys. Lett.*, vol. 106, doi: 10.1063/1.4919762, 2015.
- [7] A. Wacker, "Gain in quantum cascade lasers and superlattices: A quantum transport theory," *Phys. Rev. B*, vol. 66, no. 8, art. no. 085326 (8p.), 2002.
- [8] A. Evans, S. R. Darvish, S. Slivken, J. Nguyen, Y. Bai, and M. Razeghi, "Buried heterostructure quantum cascade lasers with high continuous-wave wall plug efficiency," *Appl. Phys. Lett.*, vol. 91, art. 071101, 2007.
- [9] J. Faist, F. Capasso, C. Sirtori, D. L. Sivco, A. L. Hutchinson, M. S. Hybertsen, and A. Y. Cho, "Quantum Cascade Lasers without Intersubband Population Inversion," *Phys. Rev. Lett.*, vol. 76, no. 3, pp. 411-414, Jan. 1996.